

## Supporting Information

### **Polyoxometalates with Tunable Third-order Nonlinear Optical and Superbroadband Optical Limiting Properties**

Long-Sheng Wang\*<sup>a,e</sup>, Yue Wang<sup>a,b</sup>, Chun-Lin Lv<sup>c</sup>, Chao Guo<sup>a</sup>, Fang-Yuan Xing<sup>b</sup>,  
Yu-Jia Dong<sup>a</sup>, Zheng Xie\*<sup>b</sup>, Shu-Yun Zhou<sup>b</sup> and Yong-Ge Wei\*<sup>d</sup>

<sup>a</sup> School of Material and Chemical Engineering, Hubei Provincial Key Laboratory of Green Materials for Light Industry, Hubei University of Technology, Hubei province, Wuhan, 430068, P.R. China. Email: [wls@mail.tsinghua.edu.cn](mailto:wls@mail.tsinghua.edu.cn)

<sup>b</sup> Key Laboratory of Photochemical Conversion and Optoelectronic Materials, Technical Institute of Physics and Chemistry, Chinese Academy of Sciences, Beijing, 100190, China. Email: [zhengxie@mail.ipc.ac.cn](mailto:zhengxie@mail.ipc.ac.cn)

<sup>c</sup> Department of Chemistry, School of Life and Environmental Sciences, Minzu University of China, Beijing, 100081, China.

<sup>d</sup> Key Lab of Organic Optoelectronics & Molecular Engineering of Ministry of Education, Department of Chemistry, School of Science, Tsinghua University, Beijing, 100084, China. Email: [yonggewei@mail.tsinghua.edu.cn](mailto:yonggewei@mail.tsinghua.edu.cn)

<sup>e</sup> State Key Laboratory of structural chemistry, Fujian Institute of Research on the Structure of Matter, Chinese Academy of Sciences, Fujian province, Fuzhou, 350002, China.

**Table S1** Crystal data collection and structure refinement parameters of  $V_1Mo_5$ ,  $V_8Mo_2$  and  $V_9Mo_1$ .

**Table S2** Selected bond lengths and bond angles of  $V_1Mo_5$ ,  $V_8Mo_2$  and  $V_9Mo_1$ .

**Table S3** BVS results of  $V_1Mo_5$ .

**Table S4** BVS results of  $V_8Mo_2$

**Table S5** BVS results of  $V_9Mo_1$ .

**Table S6** Inductively Coupled Plasma Mass Spectrometry (ICP-MS) of  $V_1Mo_5$ ,  $V_8Mo_2$  and  $V_9Mo_1$ .

**Figure S1-S3** Raman spectra of  $V_1Mo_5$ ,  $V_8Mo_2$  and  $V_9Mo_1$ .

**Figure S4** HR MS spectrum (positive region) of  $V_1Mo_5$ .

**Figure S5** HR MS spectrum (negative region) of  $V_1Mo_5$ .

**Table S7** Summary of HR MS results for  $V_1Mo_5$ .

**Figure S6** HR MS spectrum (positive mode) of  $V_8Mo_2$ .

**Figure S7** HR MS spectrum (negative mode) of  $V_8Mo_2$ .

**Table S8** Summary of GC-HRMS results for  $V_8Mo_2$ .

**Figure S8** HR MS spectrum (positive mode) of  $V_9Mo_1$ .

**Figure S9** HR MS spectrum (negative mode) of  $V_9Mo_1$ .

**Table S9** Summary of HR MS results for  $V_9Mo_1$ .

**Figure S10** XPS spectrum of  $V_1Mo_5$ .

**Figure S11** XPS spectrum of  $V_8Mo_2$ .

**Figure S12** XPS spectrum of  $V_9Mo_1$ .

**Figure S13** SEM images of  $V_1Mo_5$ ,  $V_8Mo_2$  and  $V_9Mo_1$ .

**Figure S14** TEM images of  $V_8Mo_2$ .

**Figure S15** The closed-aperture Z-scan result of  $V_1Mo_5$  and  $V_8Mo_2$ .

**Table S10** NLO coefficients of  $V_1Mo_5$ ,  $V_8Mo_2$ ,  $V_9Mo_1$  and  $V_{10}$  in propanetriol at the laser of 532 and 1064 nm.

#### **Calculation Details of NLO Coefficients**

**Figure S11.** TG and DTG curves of  $V_1Mo_5$ ,  $V_8Mo_2$  and  $V_9Mo_1$ .

**Table S1.** Crystal data collection and structure refinement parameters of **V<sub>1</sub>Mo<sub>5</sub>**, **V<sub>8</sub>Mo<sub>2</sub>** and **V<sub>9</sub>Mo<sub>1</sub>**.

	<b>V<sub>1</sub>Mo<sub>5</sub></b>	<b>V<sub>8</sub>Mo<sub>2</sub></b>	<b>V<sub>9</sub>Mo<sub>1</sub></b>
Empirical formula	C <sub>48</sub> H <sub>108</sub> N <sub>3</sub> O <sub>19</sub> Mo <sub>5</sub> V	C <sub>68</sub> H <sub>150</sub> N <sub>6</sub> O <sub>28</sub> Mo <sub>2</sub> V <sub>8</sub>	C <sub>68</sub> H <sub>151</sub> N <sub>6</sub> O <sub>28</sub> MoV <sub>9</sub>
Formula weight	1562.015	2099.34	2055.34
Crystal description	yellow, block	yellow, block	orange, block
Temperature(K)	298(2)	150(2)	150(2)
Wavelength(Å)	0.71073	0.71073	0.71073
Cryst. syst.	Monoclinic	Triclinic	Triclinic
Space group	C2/c	P-1	P-1
<i>a</i> (Å)	30.146(6)	16.747(3)	16.748(3)
<i>b</i> (Å)	18.397(4)	17.427(4)	17.445(4)
<i>c</i> (Å)	27.281(6)	17.929(4)	17.931(4)
$\alpha$ (°)	90	74.18(3)	74.20(3)
$\beta$ (°)	72.366(3)	67.43(3)	67.40(3)
$\gamma$ (°)	90	74.13(3)	74.19(3)
<i>V</i> (Å <sup>3</sup> )	13987(5)	4564.1(17)	4570.1(17)
<i>Z</i>	4	2	2
$\rho_{\text{calc}}/\text{g}\cdot\text{cm}^{-3}$	1.484	1.528	1.493
$2\theta$ range /deg	0.993 - 27.48	0.978 - 25.40	1.34 - 26.37
$\mu$ (mm <sup>-1</sup> )	1.058	1.118	1.081
<i>F</i> (000)	6416	2184	2146
Reflns. collec.	62931	44966	45574
Data/Parameters	15897/694	16444/1106	18623/1016
R(int)	0.0310	0.0640	0.0450
R <sup>a</sup> /R <sub>w</sub> <sup>b</sup>	0.0430/ 0.1449	0.0720/0.2114	0.0728/ 0.1893
GOF ( <i>F</i> <sub>2</sub> )	1.075	1.023	1.081
CCDC NO.	2080750	2080751	2080752

**Table S2.** Selected bond lengths and bond angles of **V<sub>1</sub>Mo<sub>5</sub>**, **V<sub>8</sub>Mo<sub>2</sub>** and **V<sub>9</sub>Mo<sub>1</sub>**.

	<b>V<sub>1</sub>Mo<sub>5</sub></b>	(TBA) <sub>2</sub> [Mo <sub>6</sub> O <sub>19</sub> ]
M=O(Å)	1.664(3) ~ 1.683(3)	1.674(3) ~ 1.680(3)
M-μ <sub>2</sub> -O(Å)	1.875(2) ~ 1.957(3)	1.904(3) ~ 1.942(3)
M-μ <sub>6</sub> -O(Å)	2.296(2) ~ 2.3088(5)	2.307(2) ~ 2.326(2)
M···M(Å)	3.239 ~ 3.274	3.269 ~ 3.285

	<b>V<sub>8</sub>Mo<sub>2</sub></b>	<b>V<sub>9</sub>Mo<sub>1</sub></b>	(TBA) <sub>3</sub> [H <sub>3</sub> V <sub>10</sub> O <sub>28</sub> ]
V=O(Å)	1.596(3) ~ 1.603(3)	1.591(3) ~ 1.601(4)	1.595(6) ~ 1.623(4)
M=O(Å)	1.606(4) ~ 1.615(4)	1.607(4) ~ 1.625(4)	—
M-μ <sub>2</sub> -O(Å)	1.803(3) ~ 1.897(3)	1.804(3) ~ 2.000(3)	1.814(3) ~ 2.030(2)
M-μ <sub>3</sub> -O(Å)	1.682(3) ~ 1.689(3)	1.680(3) ~ 1.691(3)	1.939(9) ~ 2.098(5)
M-μ <sub>3</sub> -O(Å)	1.921(3) ~ 2.024(3)	2.023(3) ~ 2.054(3)	—
M-μ <sub>6</sub> -O(Å)	2.089(3) ~ 2.339(3)	2.093(3) ~ 2.341(3)	2.064(1) ~ 2.349(3)
M···M(Å)	3.0642(12)~3.1989(11)	3.0627(11)~3.1557(17)	3.072(5)~3.247(9)

**Table S3.** BVS results of  $V_1Mo_5$ .

Compound	$V_1Mo_5$					
	VMo1	VMo2	VMo3	VMo4	VMo5	VMo6
<b>O(1)</b>	1.87			<b>O(11)</b>	1.92	
<b>O(2)</b>		1.9		<b>O(12)</b>		1.83
<b>O(3)</b>			1.99	<b>O(13)</b>		1.88
<b>O(4)</b>	0.86	0.81		<b>O(14)</b>	0.81	0.94
<b>O(5)</b>	0.93		0.78	<b>O(15)</b>	0.84	0.91
<b>O(6)</b>	0.82		0.93	<b>O(16)</b>	0.91	0.86
<b>O(7)</b>	0.80	0.94		<b>O(17)</b>	0.93	0.8
<b>O(8)</b>		0.77	0.97	<b>O(18)</b>		0.84
<b>O(9)</b>		0.99	0.77	<b>O(19)</b>		0.86
<b>O(10)</b>	0.29	0.29	0.30	<b>O(20)</b>		0.89
				<b>O(21)</b>	0.30	0.30
$\Sigma s$	5.57	5.7	5.74		5.71	5.63
						5.66

**Table S4.** BVS results of  $V_8Mo_2$ 

Compound	$V_8Mo_2$									
	V1	V2	VMo3	VMo4	VMo5	V6	V7	VMo8	VMo9	VMo10
<b>O(1)</b>	1.78				<b>O(15)</b>	1.76				0.49
<b>O(2)</b>		1.78			<b>O(16)</b>		1.74			
<b>O(3)</b>			1.98		<b>O(17)</b>			1.95		
<b>O(4)</b>				2.02	<b>O(18)</b>				2	
<b>O(5)</b>	0.89	0.95			<b>O(19)</b>	0.89	0.96			
<b>O(6)</b>	0.75		0.89		0.47	<b>O(20)</b>	0.65		0.9	
<b>O(7)</b>	0.78			0.92		<b>O(21)</b>	0.85		0.95	
<b>O(8)</b>	0.55				1.55	<b>O(22)</b>	0.54			1.53
<b>O(9)</b>		0.75	1.08			<b>O(23)</b>		0.69	1.07	
<b>O(10)</b>		0.5			1.57	<b>O(24)</b>		0.83		1.03
<b>O(11)</b>		0.76		1.07		<b>O(25)</b>		0.54		1.55
<b>O(12)</b>			0.57	0.62	0.77	<b>O(26)</b>			0.57	0.63
<b>O(13)</b>	0.26	0.26	0.32	0.3	0.48	<b>O(27)</b>	0.26	0.27	0.31	0.29
<b>O(14)</b>			0.63	0.58	0.73	<b>O(28)</b>			0.61	0.63
$\Sigma s$	5.01	5	5.47	5.51	5.57		4.95	5.03	5.41	5.53
										5.49

**Table S5.** BVS results of **V<sub>9</sub>Mo<sub>1</sub>**.

Compound	<b>V<sub>9</sub>Mo<sub>1</sub></b>										
	V1	V2	VMo3	VMo4	V5	V6	V7	VMo8	VMo9	V10	
<b>O(1)</b>	1.8					<b>O(21)</b>	1.76			0.44	
<b>O(2)</b>		1.81				<b>O(22)</b>		1.74			
<b>O(3)</b>			1.9			<b>O(23)</b>			1.82		
<b>O(4)</b>				1.93		<b>O(24)</b>				1.87	
<b>O(5)</b>	0.88	0.95				<b>O(25)</b>	0.9	0.93			
<b>O(6)</b>	0.74		0.84		0.44	<b>O(26)</b>	0.64		0.86		
<b>O(7)</b>	0.78			0.91		<b>O(27)</b>	0.88			0.9	
<b>O(8)</b>	0.54				1.35	<b>O(28)</b>	0.53			1.33	
<b>O(9)</b>		0.76	1.02			<b>O(29)</b>		0.68	1.05		
<b>O(10)</b>		0.76		1.02		<b>O(30)</b>		0.76		1.01	
<b>O(11)</b>		0.5			1.36	<b>O(31)</b>		0.53		1.38	
<b>O(12)</b>			0.55	0.61	0.7	<b>O(32)</b>			0.56	0.61	
<b>O(13)</b>			0.64	0.56	0.67	<b>O(33)</b>			0.61	0.6	
<b>O(14)</b>	0.27	0.26	0.32	0.3	0.45	<b>O(34)</b>	0.26	0.28	0.31	0.29	

**Table S6.** Inductively Coupled Plasma Mass Spectrometry (ICP-MS) of **V<sub>1</sub>Mo<sub>5</sub>**, **V<sub>8</sub>Mo<sub>2</sub>** and **V<sub>9</sub>Mo<sub>1</sub>**. (The atom number ratio of V and Mo in vanadomolybdic acid for ICP measurement)

Sample	Concentration/M <sub>Mo</sub> (ppm)	Concentration/M <sub>V</sub> (ppm)	Atomic number ratio V/Mo
<b>V<sub>1</sub>Mo<sub>5</sub></b>	0.099	0.020	0.20
<b>V<sub>8</sub>Mo<sub>2</sub></b>	0.014	0.056	4.00
<b>V<sub>9</sub>Mo<sub>1</sub></b>	0.012	0.111	9.25

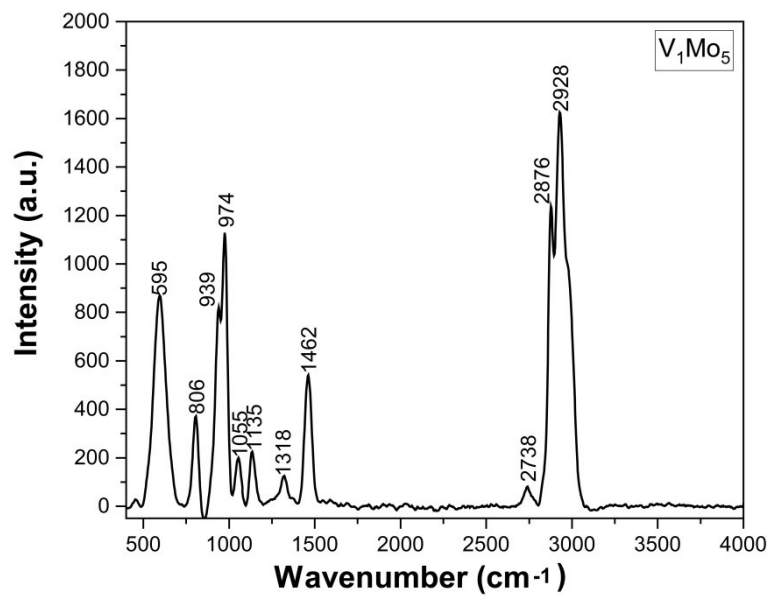


**Figure S1.** Raman spectrum of  $V_1Mo_5$ .

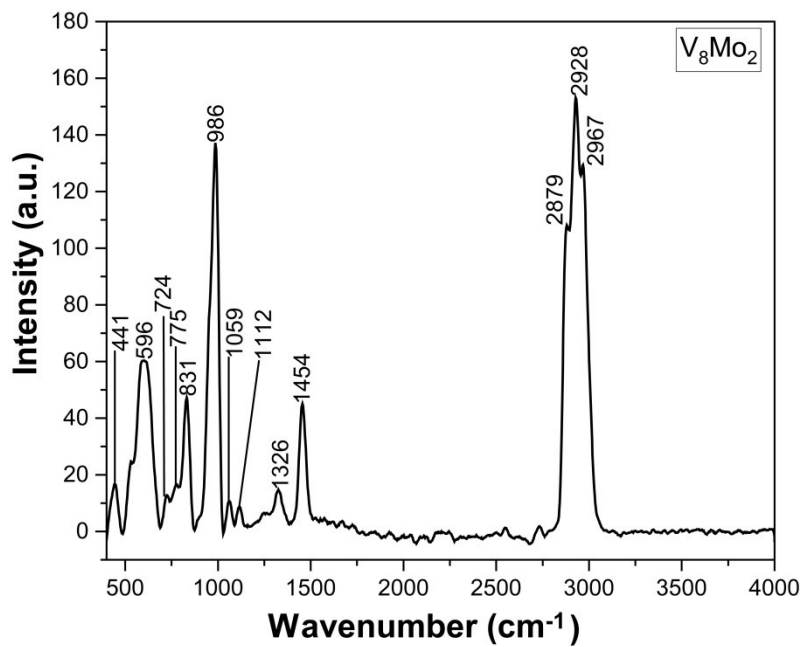


**Figure S2.** Raman spectrum of  $V_8Mo_8$ .

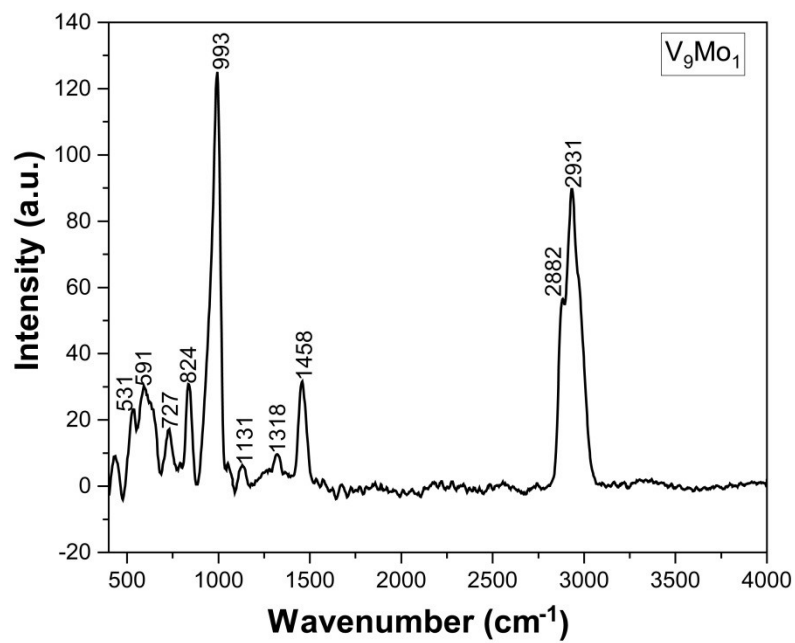
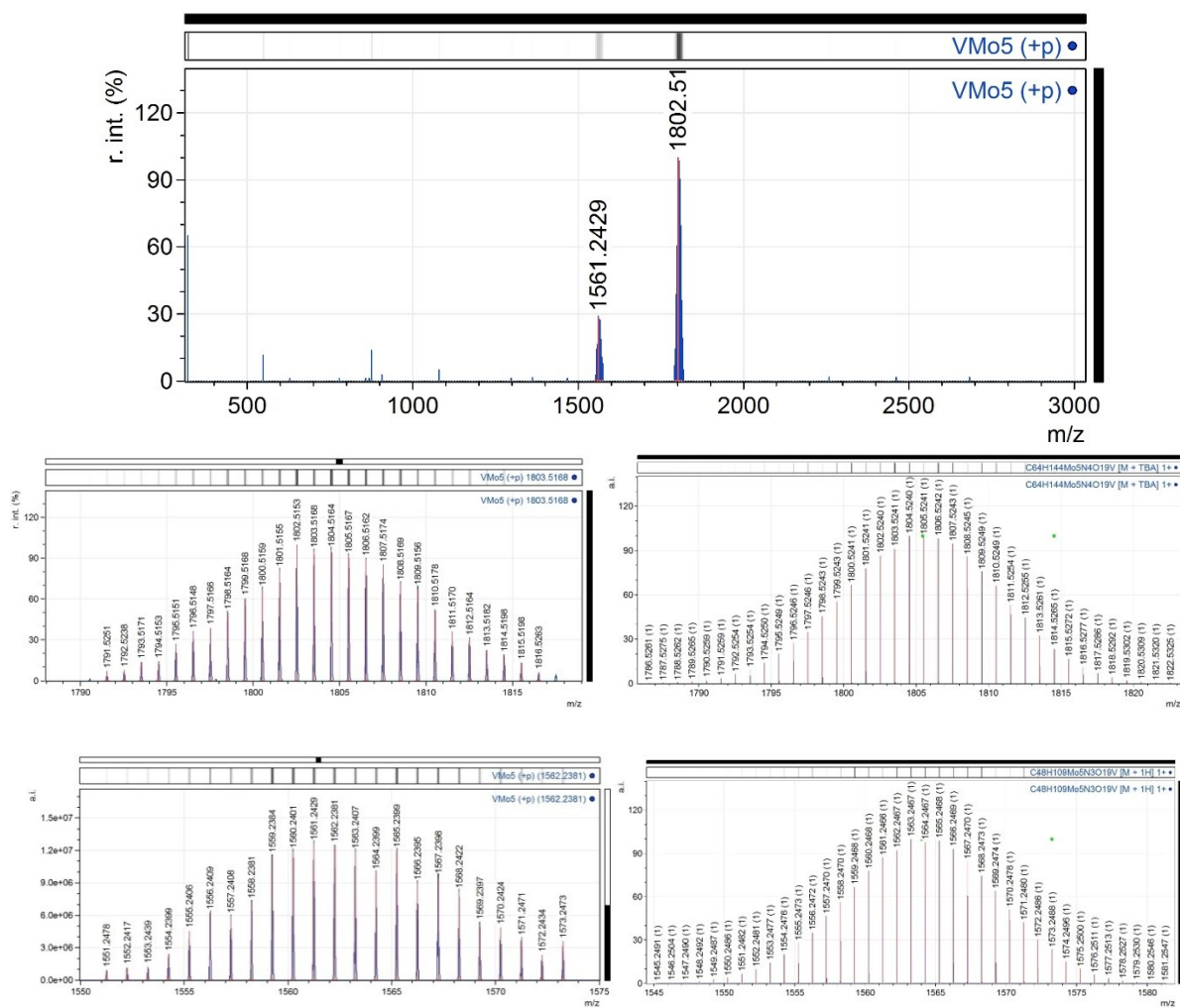
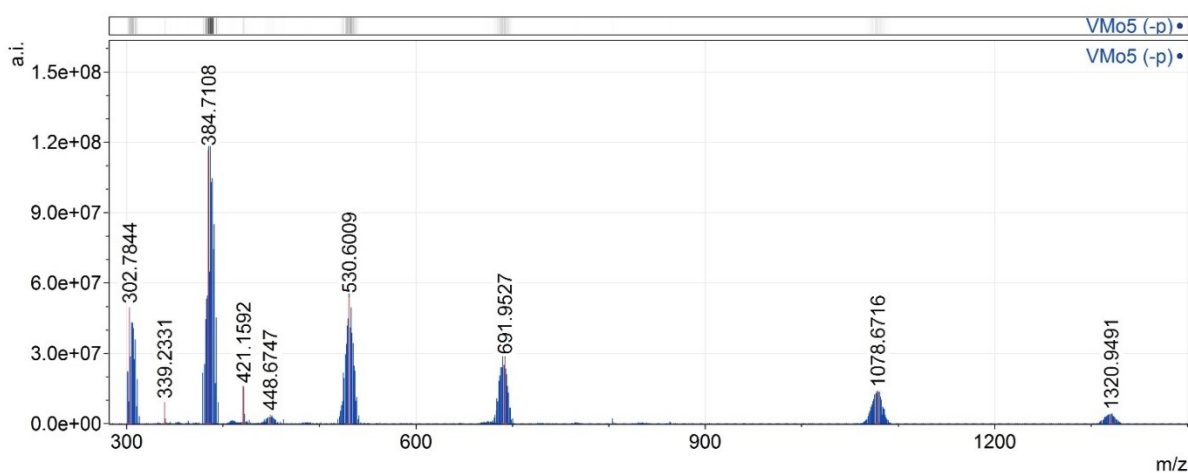


Figure S3. Raman spectrum of  $V_9Mo_1$ .





**Figure S4.** GC-HRMS spectrum (positive region) of  $V_1Mo_5$ : 1561.2429 for  $\{M + 1H\}^{1+}$ , calcd. 1562.2467; 1803.5168 for  $\{M + 1TBA\}^{1+}$ , calcd. 1803.5241.



**Figure S5.** GC-HRMS spectrum (negative region) of  $V_1Mo_5$ : 1320.9491 for  $\{M - TBA\}^{1-}$ ; calcd. 1320.946; 1078.6716 for  $\{M - 2TBA + H\}^{1-}$ ; calcd. 1078.669.

**Table S7** Summary of HR MS results of  $V_1Mo_5$ .

Negative mode of HRMS for $V_1Mo_5$				
m/z	Calculated m/z	Assigned Species	Charge	Notes
302.7844	302.784	{HMo <sub>2</sub> O <sub>7</sub> } <sup>1-</sup>	-1	fragment
384.7108	384.710	{VMo <sub>2</sub> O <sub>9</sub> } <sup>1-</sup>	-1	fragment
421.1592	426.68	{Mo <sub>3</sub> O <sub>11</sub> } <sup>1-</sup>	-1	fragment
448.6747	448.674	{HMo <sub>3</sub> O <sub>10</sub> } <sup>1-</sup>	-1	fragment
530.6009	530.600	{VMo <sub>3</sub> O <sub>12</sub> } <sup>1-</sup>	-1	fragment
691.9527	691.951	{TBA(Mo <sub>3</sub> O <sub>10</sub> )} <sup>1-</sup>	-1	fragment
1078.6716	1078.669	{M- 2TBA + H} <sup>1-</sup>	-1	molecule ion
1320.9491	1320.946	{M- TBA} <sup>1-</sup>	-1	molecule ion
Positive mode of HRMS for $V_1Mo_5$				
1564.2419	1564.2467	{M + 1H} <sup>1+</sup>	+1	molecule ion
1806.5134	1806.5242	{M + 1TBA} <sup>1+</sup>	+1	molecule ion

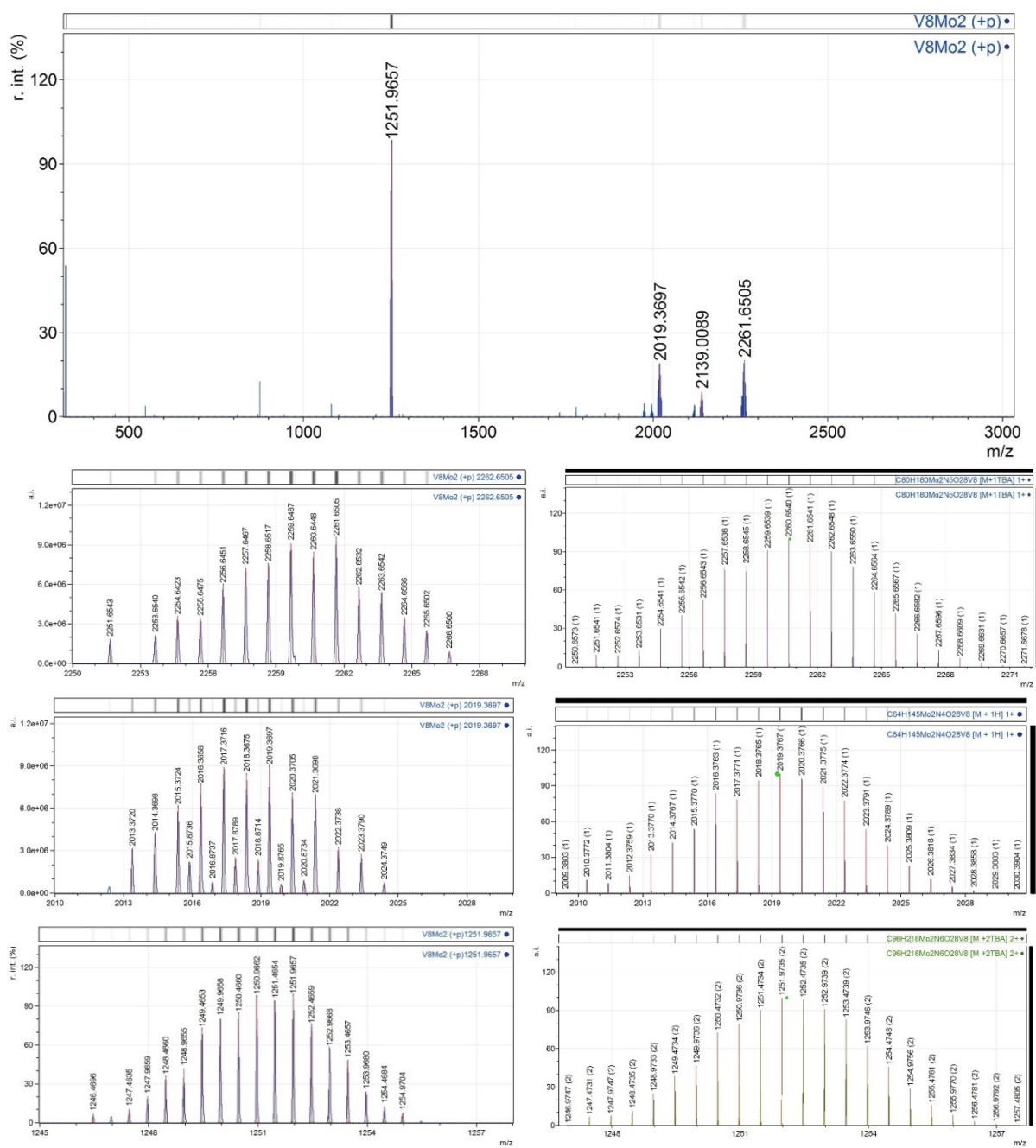


**Figure S6.** HRMS spectrum (positive mode) of  $V_8Mo_2$ : 1250.9656 for  $\{M + 2TBA\}^{2+}$ , calcd. 1250.9736; 2018.3716 for  $\{M + 1H\}^{1+}$ , calcd. 2018.3765; 2261.6596 for  $\{M + 1TBA\}^{1+}$ ; calcd. 2261.6541.

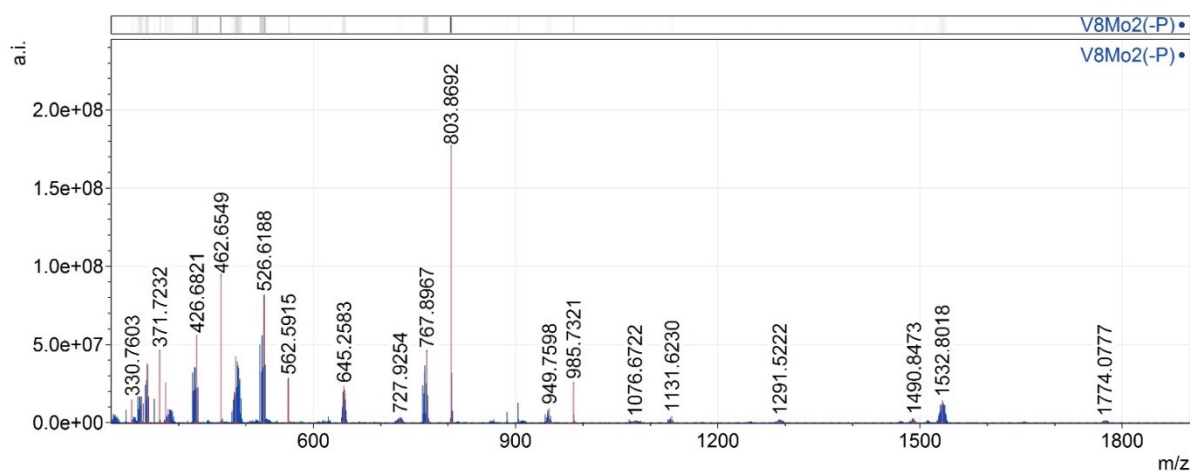


**Figure S7.** HRMS spectrum (negative mode) of  $V_8Mo_2$ : 1774.0777 for  $\{M - TBA\}^{1-}$ , calcd. 1774.076; 1532.8018 for  $\{M - 2TBA + H\}^{1-}$ , calcd. 1532.799; 1291.5122 for  $\{M - 3TBA + 2H\}^{1-}$ , calcd. 1291.522.

**Table S8** Summary of HR MS results for  $V_8Mo_2$ .

HR MS Negative mode of $V_8Mo_2$				
m/z	Calculated m/z	Assigned Species	Charge	Notes
334.7561	334.755	$\{HV_2MoO_9\}^{1-}$	-1	fragment
384.7107	384.710	$\{VMo_2O_9\}^{1-}$	-1	fragment
426.6821	426.681	$\{V_3MoO_{11}\}^{1-}$	-1	fragment
462.6549	462.654	$\{V_5O_{13}\}^{1-}$	-1	fragment
484.6474	484.646	$\{HV_2Mo_2O_{12}\}$	-1	fragment
526.6188	526.625	$\{M - 4TBA + 2H\}^{2-}$	-2	molecule ion
645.2583	646.264	$\{M - 3TBA + H\}^{2-}$	-2	molecule ion
766.3977	766.430	$\{V_5Mo_2O_{20}\}^{1-}$	-1	fragment
767.8967	767.903	$\{M - 2TBA\}^{2-}$	-1	molecule ion
867.8346	867.366	$\{HV_6Mo_2O_{23}\}^{1-}$	-1	fragment
949.7598	949.463	$\{HV_7Mo_2O_{25}\}^{1-}$	-1	fragment
1076.6722	1076.226	$\{M - 4TBA + 2H + Na\}^{1-}$	-1	molecule ion
1291.5122	1291.522	$\{M - 3TBA + 2H\}^{1-}$	-1	molecule ion
1532.8018	1532.799	$\{M - 2TBA + H\}^{1-}$	-1	molecule ion
1774.0777	1774.076	$\{M - TBA\}^{1-}$	-1	molecule ion
HR MS positive mode of $V_8Mo_2$				
m/z	Calculated m/z	Assigned Species	Charge	Notes
1250.9656	1250.9736	$\{M + 2TBA\}^{2+}$	+2	molecule ion
2018.3716	2018.3765	$\{M + 1H\}^{1+}$	+1	molecule ion
2261.6596	2261.6541	$\{M + 1TBA\}^{1+}$	+1	molecule ion

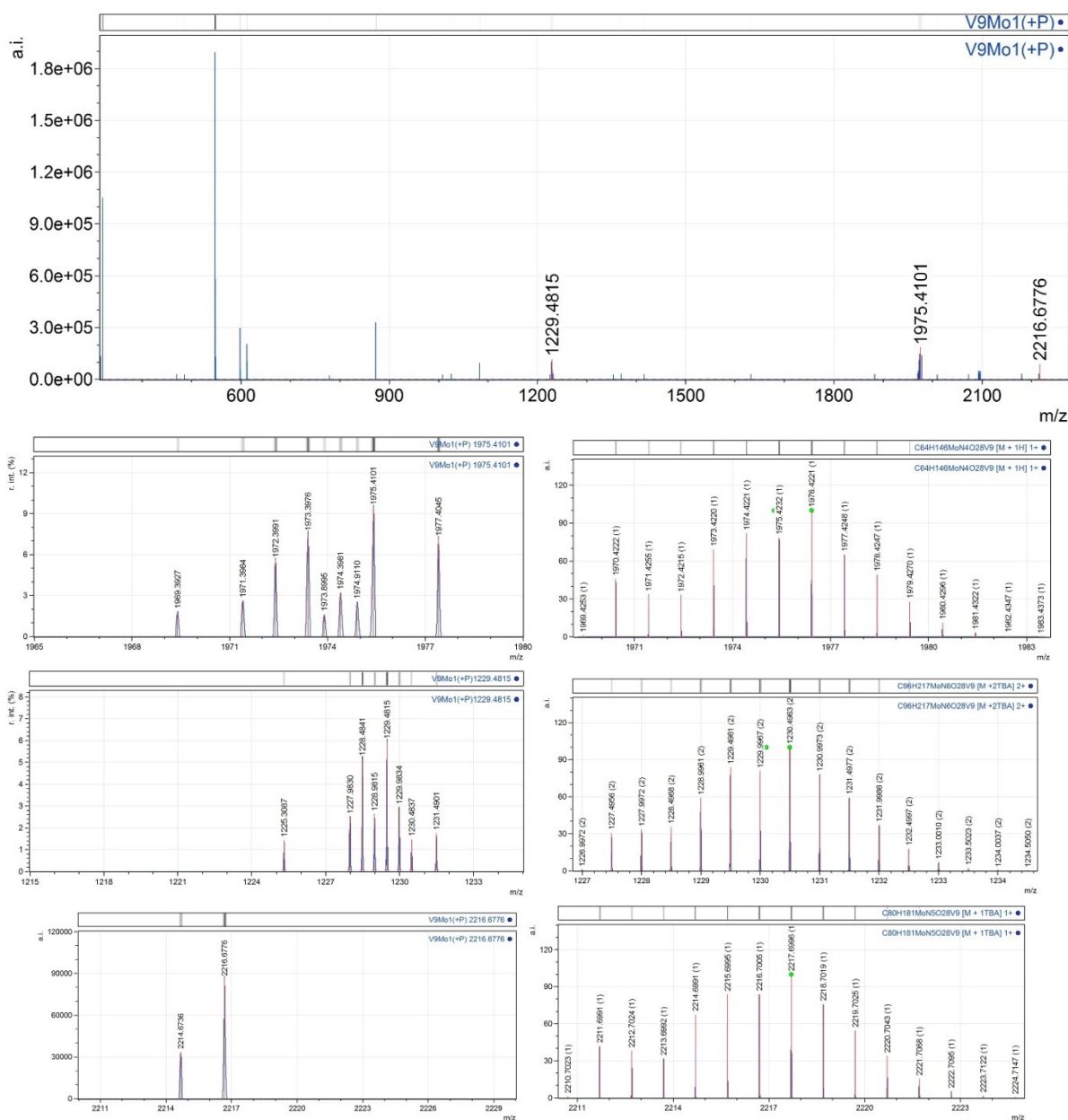


**Figure S8.** HR MS spectrum (positive mode) of  $V_9Mo_1$ : 1229.4815 for  $\{M + 2TBA\}^{2+}$ , calcd. 1229.1961; 1975.4501 for  $\{M + H\}^+$ , calcd. 1975.4231; 2216.6776 for  $\{M + TBA\}^+$ , calcd. 2216.7005.

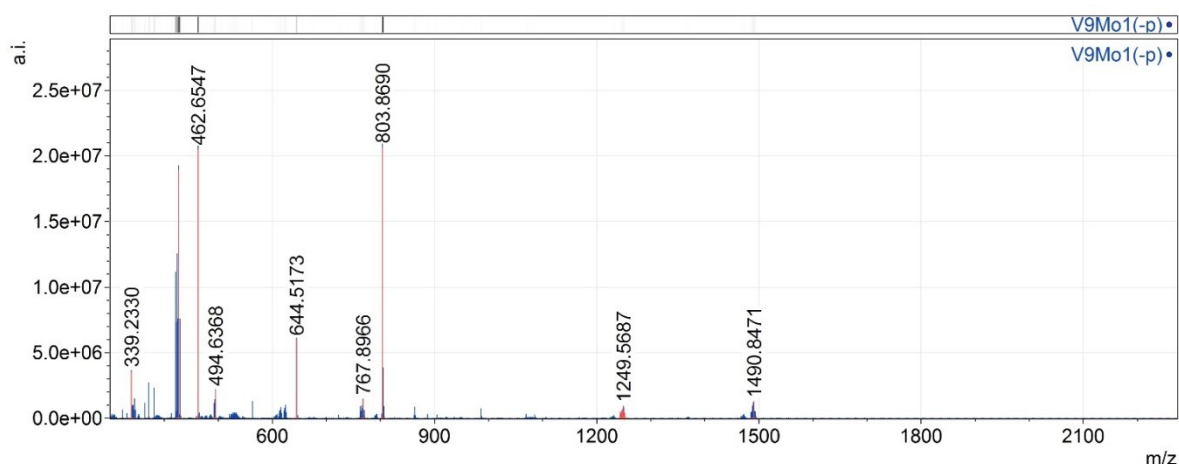


**Figure S9.** HR MS spectrum (negative mode) of  $V_9Mo_1$ : 1490.8471 for  $\{M-2TBA+H\}^{1-}$ , calcd. 1490.8485; 1249.5687 for  $\{M-3TBA+2H\}^{1-}$ , calcd. 1249.5673.

**Table S9** Summary of HR MS results for  $V_9Mo_1$ .

HR MS Negative mode of $V_9Mo_1$				
m/z	Calculated m/z	Assigned Species	Charge	Notes
339.2330	339.760	$\{HV_2MoO_9\}^{1-}$	-1	ragment
426.6818	426.68	$\{V_3MoO_{11}\}^{1-}$	-1	fragment
462.6547	462.65	$\{V_5O_{13}\}^{1-}$	-1	fragment
494.6368	494.628	$\{HV_4MoO_{12}\}$	-1	fragment
644.5173	644.516	$\{V_7O_{18}\}^{1-}$	-1	fragment
1249.5687	1249.5673	$\{M-3TBA+2H\}^{1-}$	-1	molecule ion
1490.8471	1490.8485	$\{M-2TBA+H\}^{1-}$	-1	molecule ion
HR MS Negative mode of $V_9Mo_1$				
m/z	Calculated m/z	Assigned Species	Charge	Notes
1229.4815	1229.1961	$\{M+2TBA\}^{2+}$	+2	molecule ion
1975.4501	1975.4231	$\{M+H\}^{1+}$	+1	molecule ion
2216.6776	2216.7005	$\{M+TBA\}^{1+}$	+1	molecule ion

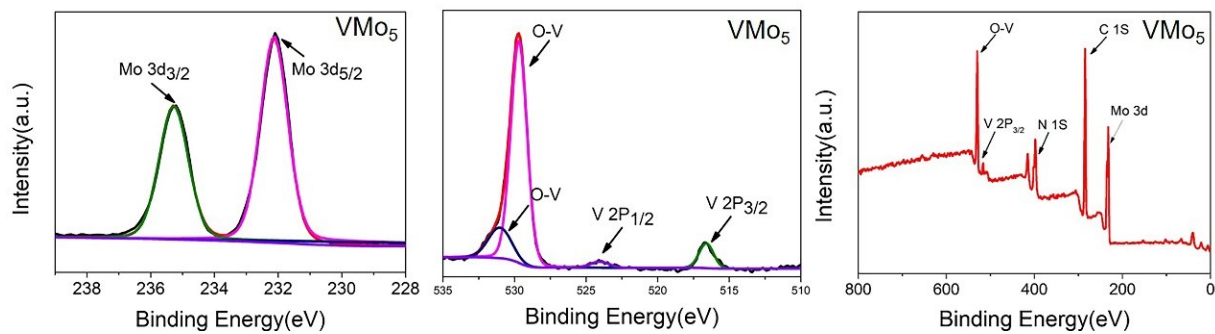


**Figure S10.** XPS spectrum of  $V_1Mo_5$ .

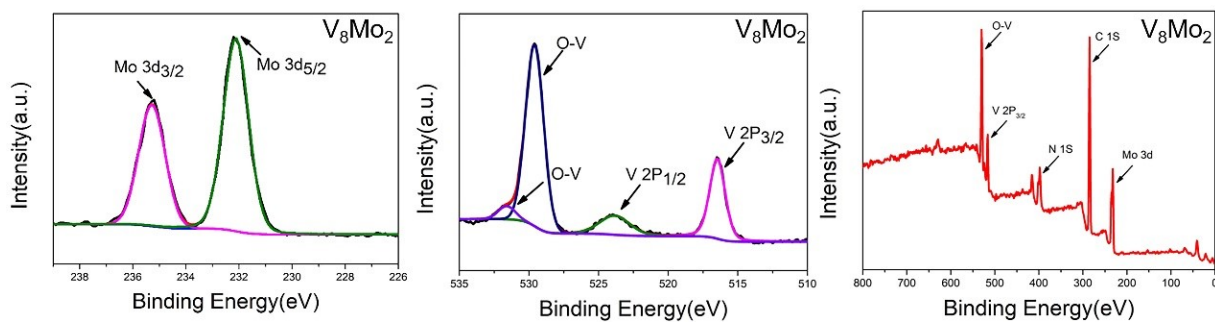


**Figure S11.** XPS spectrum of  $V_8Mo_2$ .

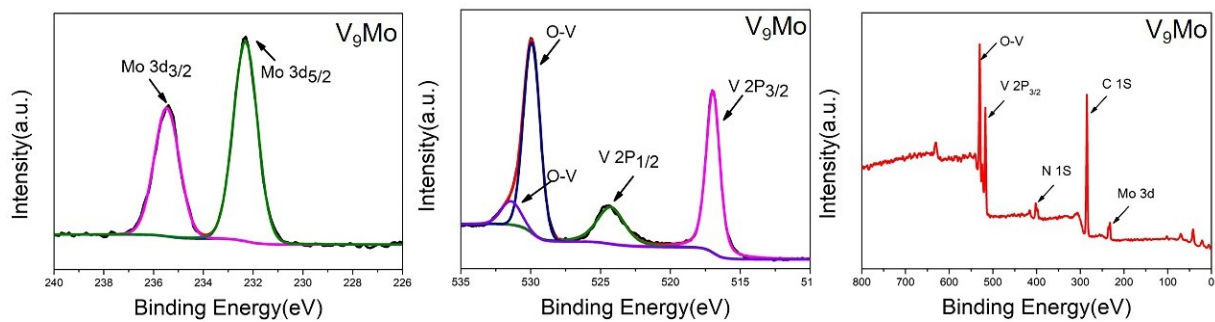


**Figure S12.** XPS spectrum of  $V_9Mo_1$ .

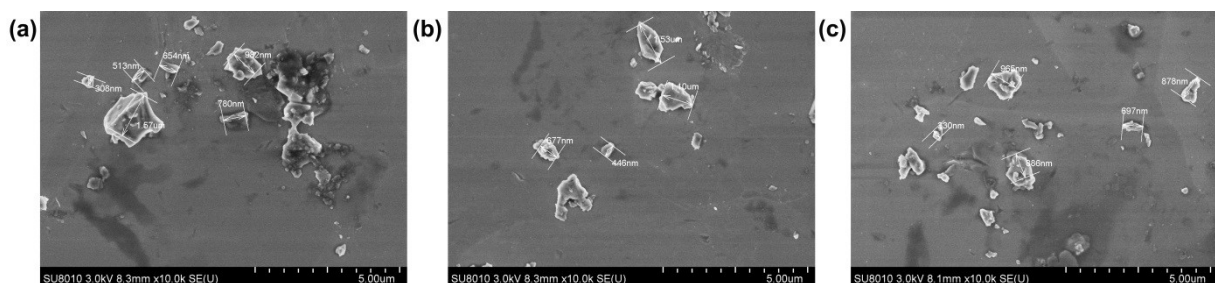


**Figure S13.** SEM images of  $V_1Mo_5$ ,  $V_8Mo_2$  and  $V_9Mo_1$ .

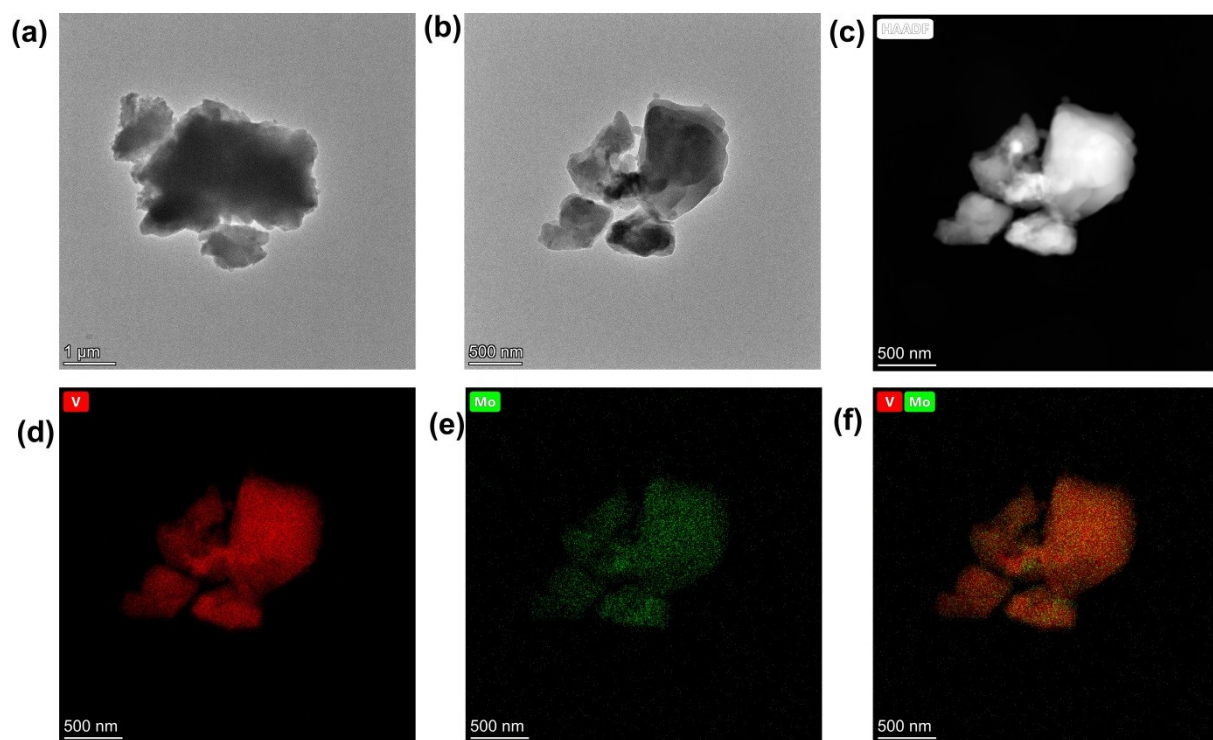


**Figure S14.** TEM images of  $V_8Mo_2$ : (a), (b) TEM images, (c) HAADF-STEM image; (d) Corresponding EDX mapping of V and Mo distribution; (f) composite of V/ Mo.



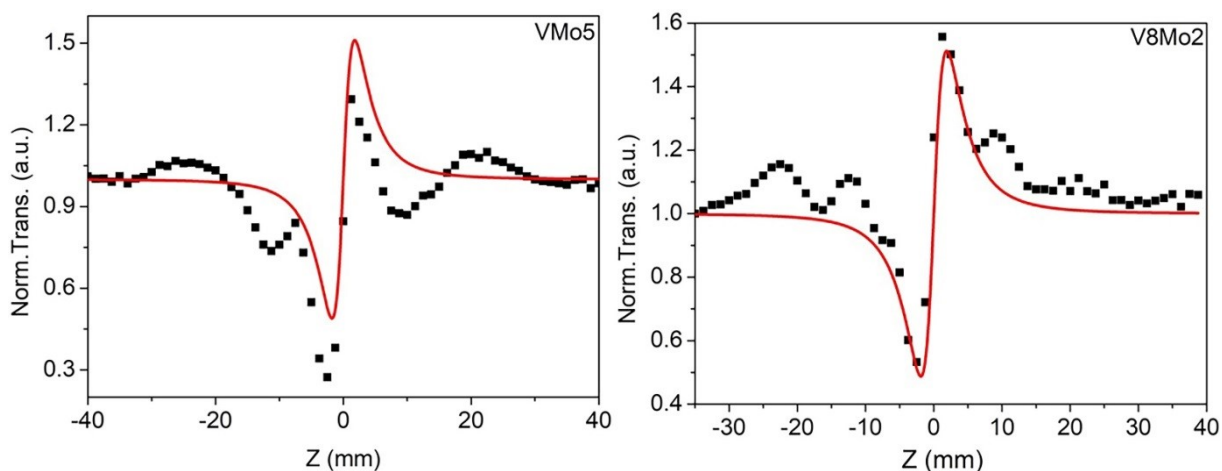


**Figure S15.** The closed-aperture Z-scan result of  $V_1Mo_5$  and  $V_8Mo_2$ .

**Table S10.** NLO coefficients of  $V_{10}$ ,  $V_1Mo_5$ ,  $V_8Mo_2$  and  $V_9Mo_1$  in propanetriol at the laser of 532 and 1064 nm.

Compounds	$\lambda$ [nm]	$T_{min}$	$\beta_{eff}$ [cm GW <sup>-1</sup> ]	Im $\chi(3)$ [esu]	$n_2$
$V_1Mo_5$	532	0.75	60.16	$2.9 \times 10^{-8}$	$1.08 \times 10^{-5}$
$V_8Mo_2$		0.50	123.79	$6.0 \times 10^{-8}$	$8.9 \times 10^{-6}$
$V_9Mo_1$		0.06	691.79	$3.3 \times 10^{-7}$	$9.95 \times 10^{-6}$
$V_{10}$		0.26	202.63	$9.8 \times 10^{-8}$	
$V_1Mo_5$	1064	0.85	80.19	$7.8 \times 10^{-8}$	
$V_8Mo_2$		0.53	127.98	$1.24 \times 10^{-7}$	
$V_9Mo_1$		0.22	292.52	$2.8 \times 10^{-7}$	
$V_{10}$		0.80	69.59	$6.8 \times 10^{-8}$	

### Calculation Details of NLO Coefficients

The measured Z-scan curves were fitted using the following expressions: <sup>[3]</sup>

$$T(z) = 1 - \beta I_0 L_{eff} / [2\sqrt{2} \left(1 + \frac{z^2}{z_0^2}\right)] = 1 - [1 - T(z=0)] / \left(1 + \frac{z^2}{z_0^2}\right)$$

$$L_{eff} = [1 - \exp(-\alpha L)] / \alpha$$

Where  $\beta$  is nonlinear absorption coefficient,  $I_0$  is the energy density at the focus ( $z=0$ ),  $L_{eff}$  is the effective thickness of the sample;  $\alpha$  is the linear absorption coefficient and  $L$  is the thickness of sample. The equation of  $T$  can be fitted and calculated to get the  $\beta$  values.

The imaginary parts of the third order nonlinear optical susceptibility  $\chi^{(3)}$  are determined from the following equation: <sup>[4]</sup>

$$\text{Im } \chi^{(3)} = \frac{n_0^2 \epsilon_0 c \lambda \beta}{2\pi}$$

where  $n_0$  is the linear refractive index,  $\epsilon_0$  is the permittivity of free space,  $c$  is the speed of light,  $\lambda$  is the laser wavelength and  $\beta$  is nonlinear absorption coefficient.

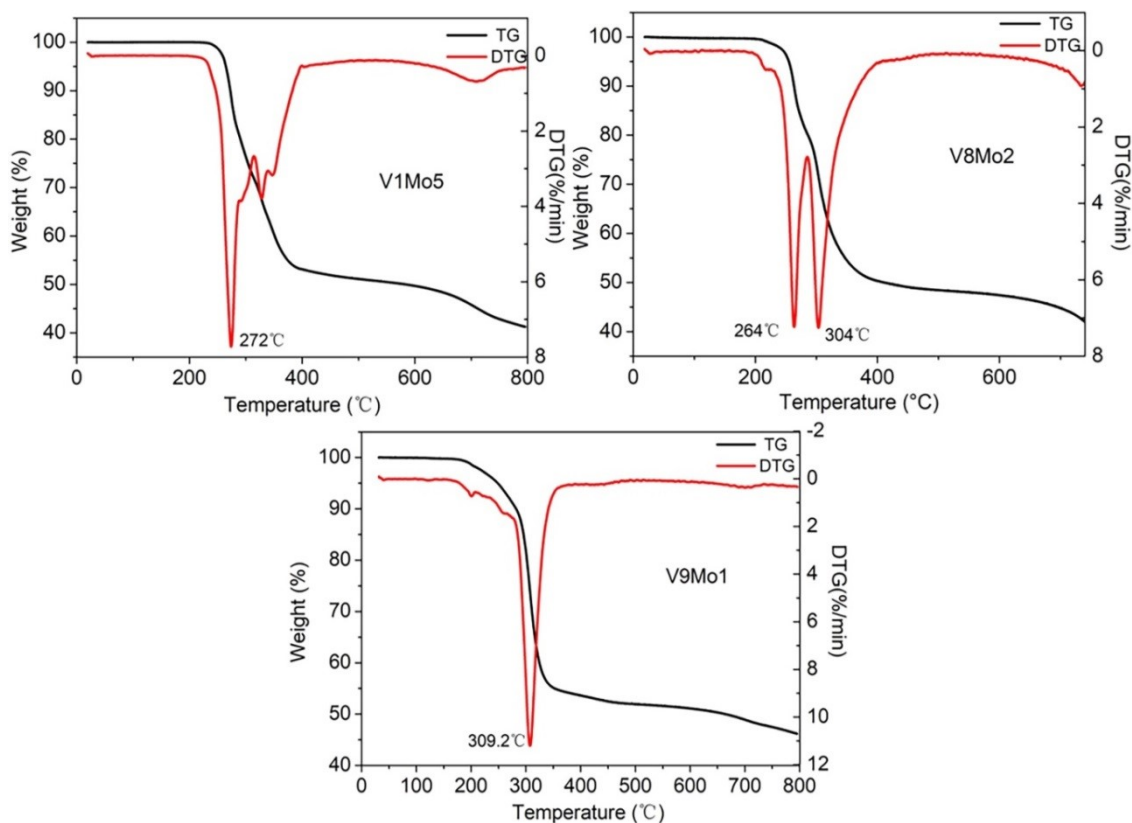


**Figure S17.** TG and DTG curves of  $V_1Mo_5$ ,  $V_8Mo_2$  and  $V_9Mo_1$ .

Thermo gravimetric analyzer (TGA) was applied to explore the thermal stability of  $V_1Mo_5$ ,  $V_8Mo_2$  and  $V_9Mo_1$  using the temperature rate of 10 °C/min at the  $N_2$  atmosphere. As shown in Fig S11,  $V_1Mo_5$  has a negligible weight loss of about 0.3% before 220°C. A rapid weight loss (46.6%) occurs between 220~390°C, which is corresponding to the loss of three TBA cations (46.2%).  $V_8Mo_2$  displays a very small weight loss ca. 0.9% before 217°C, which is less than the theoretical loss of two acetonitrile solvent molecules (3.8%) because  $V_8Mo_2$  is easy to lose its crystallized solvent molecules. A rapid weight loss (48.3%) is followed between 217~390°C, which is well matched with the loss of four TBA cations (48.1%). Compound **3** has a slow weight loss before 195 °C (ca. 0.09%), which is also less than the theoretical weight loss of two acetonitrile solvent molecules (3.99%), indicating that  $V_9Mo_1$  had lost two crystallized acetonitrile molecules before the TG test. A rapid weight loss (ca. 45.3%) associated with the loss of four TBA cation (47.2%) is found between 195 ~ 395 °C.

Ref:

- [1] Z. Xie, F. Wang, C. Y. Liu, *Adv Mater* **2012**, 24, 1716.
- [2] a) G. M. Sheldrick, University of Göttingen, Germany 1997; b) G. M. Sheldrick, University of Göttingen, Germany 1997; c) G. M. Sheldrick, *Acta. Crystallographica Section A Foundations of Crystallography* **2008**, 64, 112.
- [3] M. Sheik-bahae, A. A. Said, T.-h. Wei, E. W. V. Stryland, *IEEE J. Quantum Electron.* **1990**, 26, 760.
- [4] A. A. Said, M. Sheik-Bahae, D. J. Hagan, T. H. Wei, J. Wang, J. Young, E. W. V. Stryland, *J. Opt. Soc. Am. B: Opt. Phys.* **1992**, 9, 405.